Journal of Materials and Environmental Science
ISSN : 2028-2508
CODEN : JMESCN

J. Mater. Environ. Sci., 2021, Volume 12, Issue 6, Page 787-797

http://www.jmaterenvironsci.com

Study of Pyrolysis Temperature Influence on Physicochemistry of Patchouli Biochar and Patchouli pyrolysis Reaction Using $CoCl_2$ Chemical Activator

T. Setianingsih[1*], Masruri[2], B. Ismuyanto[3]

[1]*Department of Chemistry, Brawijaya University, Malang 65145, Indonesia*
[2]*Department of Chemistry, Brawijaya University, Malang 65145, Indonesia*
**Corresponding author, Email address: tutiksetia@ub.ac.id*

Received 22 May 2021,
Revised 03 June 2021,
Accepted 06 June 2021

Keywords
- ✓ *Biochar*
- ✓ *Patchouli biomass*
- ✓ *Pyrolisis*
- ✓ *Temperature*
- ✓ *$CoCl_2$*
- ✓ *Adsorption*

tutiksetia@ub.ac.id
Phone: +62-083192813399

Abstract

Biochar was prepared from patchouli biomass using $CoCl_2$ activator with the aim to study the influence of pyrolysis temperature toward porosity and chemical surface. The biomass was pyrolyzed at five different temperatures i.e. 350, 450, 550, 650, and 750 °C. Characterizations of the afforded biochar were performed using gas sorption analysis, FTIR spectrophotometry, X-ray diffraction, and also TGA-DTA. The results give the highest porosity (micro- and mesoporous) biochars were achieved at 450 and 650 °C pyrolysis. Pyrolysis below 650 °C still retains the hydroxyl and carbonyl group. But these groups disappear at 650 °C pyrolysis with activator and at 750 °C pyrolysis without activator. Moreover, the produced biochar slightly contains graphite and amorphous structures. TGA-DTA analysis confirmed that the biomass was decomposed at a lower temperature with a lower weight loss.

1. Introduction

Biochar is a porous carbonaceous product is obtained from the pyrolysis of various organic matters. The source of organic matter is provided in relatively large quantities from local sources, for example; biological wastes, plant biomass, agricultural residues [1-4], and industrial sludge [5]. The abundance of patchouli oil plantation in Indonesia also provides an enormous source for biochar. In total, about 9600 ha plantation is established [6], and this gives a huge amount of patchouli biomass from the part of leaves, stem, wood, and branch. The wood biomass contains 44% cellulose, 25% hemicellulose, and 23% lignin [7]. The wood can be pyrolyzed to produce biochar [8]. Beside that other source of lignocellulose biomass from various agricultural biomass can also be directly used as a precursor for biochar [9,10].

The unique characters of biochar are related to the porosity and surface functional groups. These properties play an important role for many applications, such as for nanoparticle metal oxide matrix [11], adsorbent [12], electrical supercapacitor [13], and soil conditioner [14]. The performance of biochar as an adsorbent has been verified by previous researchers for adsorption of various pollutants such as heavy metals [15, 16, 17], ammonium [18], and various organic compounds [3,11,19,20,21]. Physicochemical properties such as surface area [9,22], porosity [16], and surface functional groups [9, 22] affect the

adsorption capability. For examples for adsorption of methylene blue and I_2 by biochars derived from rice straw, oak tree, and rice husk. The adsorption capacity increased by increasing of the BET surface area (S_{BET}) [9]. The adsorption capacity of benzene (using dual mode and Dubinin Astakov) and methyl tert-butyl ether (using Freundlich model) using biochar prepared from maize straw was also increased by increasing of both S_{BET} and microporous volume. And also, the involving of diminishing of the polar functional groups such as –OH, C=O and C-O [19]. The adsorption of paracetamol pollutant in water improved by declining of biochar acidity [23]. In addition to that, the physicochemical properties of biochar are also influenced by the nature of feedstock and temperature during synthesis [10, 24]. For example, the surface area (S_{BET}) of biochars which were produced from wheat straw, corn straw, and peanut shell biomass is increased by elevating the pyrolysis temperature from 400 to 600 ^oC [9,10]. Moreover, preparation in elevated temperature (from 400 to 600 ^oC) of biochar from rice husk using KOH activator give the increment of S_{BET}, micro- and mesoporous volume, and pore size, however, the important functional groups also diminish by increasing of pyrolysis temperature to above 600 ^oC [22].

To study more detailed biochar properties, the TGA-DTA commonly used to understand pyrolysis reaction during biochar's preparation. For examples for studying the thermal degradation behavior of bamboo [25]. Thermal analysis studies the behavior of biochar precursor and also to determine the temperature range of biochar's activation [26]. Meanwhile, TGA can be used to predict the activator decomposition and to find the calcination temperature during composite preparation. Some papers reported calcination of metal salt-impregnated carbon or metal oxide-impregnated carbon has changed both of the structure of carbon composite and also their adsorption capability [27, 28]. This research study the effect of pyrolysis temperature on physicochemical properties of biochar derived from patchouli biomass. Thermal analysis was also conducted to study the pyrolysis reaction. The adsorption evaluation was also undertaken to get direct explanation correlated to physicochemical properties of biochar synthesized with organic pollutants [29] such as paracetamol as the adsorbate. It is an important step in order to further application of patchouli biochar for drug wastewater treatment.

2. Methodology

2.1 *Source and preparation of source*

All chemicals which were used in for research were Merck or as other mentioned. Patchouli biomass included mixture of root and stem. The biomass was crushed and cleaned by water and dried, then sieved to get 60 - 100 mesh of solid particles.

2.2. Preparation of biochar

A 10 g of the 60-100 mesh clean biomass precursor, 17.448 g of $CoCl_2.6H_2O$, and 60 mL of the distilled water were mixed and stirred at 100 ^oC for 4 h. Then, the impregnated biomass was pyrolyzed at various temperatures (350, 450, 550, 650, and 750 ^oC) for 2 h under flowing of nitrogen gas. The activator was removed using 1.0 M of hydrochloric acid solution and distilled water. The biochar product was further characterized after conditioned in particle size of 100-120 mesh.

2.3 *Characterization of biochar*

2.3.1 *Gas Sorption Analysis*

The porosity of biochars was analyzed using gas sorption analysis method. Data of N_2 adsorption isotherm was measured at -196°C using Surface Area Analyzer (Quantachrome NovaWin2). The adsorption data were treated using BET (Brunauer Emmet Teller) and POD (Pierce Orr Dalla Vale) method to determine surface area and pore volume.

2.3.2 *FTIR spectrophotometry analysis*

Surface functional groups of biochars were determined based on FTIR spectra. It was measured using FTIR spectrophotometer (Shimadzu) with pellet KBr technique by mixing the dried biochars with an oven-dried KBr. Data of FTIR spectra were collected in a range of 400 – 4000 cm^{-1}.

2.3.3 *XRD analysis*

Crystal structure of biochar was characterized using X-ray diffractometer (PANanalytical type XPert PRO). Diffractogram patterns were recorded using CuK_{α} of 1.5445^{o} at 35 mA and 40 kV.

2.3.4 *Thermal analysis*

Pyrolisis reaction of the $CoCl_2$ impregnated in biomass was analyzed using TGA-DTA (LINSEIS STA PT 1700). The analysis was performed under argon streaming

2.4. *Adsorption test*

This adsorption test used biochar which was prepared at 450 ^{o}C. The biochar was mixed with paracetamol/ amoxicillin/tetracycline solution at ratio (mg/mL) of 4:5. The adsorption was conducted at a various concentration of adsorbate (50, 100, 150 and 200 ppm), and was shaken at 175 rpm for 24h. Drug analysis was determined by using UV-Vis spectrophotometer at each maximum wavelength of 275 nm (tetracycline), 227 nm (amoxicillin), and 243 nm (paracetamol). Calibration curves were built based on measurement of the standard solution series of 10 to 70 ppm for each tetracycline and amoxicillin, and 10 to 50 ppm for paracetamol.

3. Results and Discussion

3.1 *Pore and surface area of biochar*

Pore characteristics of biochars have been characterized and the data is reported in **Table 1.** Biochar which was produced at 350 ^{o}C has no measurable S_{BET} due to no nitrogen gas adsorption, except at P/P_o range of 0.90 – 0.99. It indicates relatively no porosity. Total pore volume (V_t) correlate to the adsorption of biochar particle intrinsic.

Table 1. Pore characteristics of biochars prepared at various pyrolysis temperatures

Temperature (^{o}C)	S_{BET} (m^2/g)	S_{meso} (m^2/g)	S_{macro} (m^2/g)	S_{micro} (m^2/g)	V_t (cm^3/g)	V_{meso} (cm^3/g)	V_{macro} (cm^3/g)	V_{micro} (cm^3/g)
350	-	-	-	-	0.16	-	-	-
450	946.87	53.35	0.31	946.72	0.16	0.06	0.01	0.05
550	331.07	189.61	0.15	330.87	0.13	0.15	0	0.10
650	354.98	229.12	1.55	354.31	0.25	0.20	0.05	0.14
750	102.07	104.81	0	101.61	0.27	0.10	0.17	0.13

V_t was calculated from data of adsorption isotherm at P/P_o = 0.99 [30]
S_{BET} was calculated from data of adsorption isotherm at P/P_o range of 0.05–0.035 using BET formula [30]
S_{meso}, V_{meso}, S_{macro}, and V_{macro} were calculated from data of desorption isotherm using POD method [30]
V_{micro} and S_{micro} was calculated from data of adsorption isotherm using *the t-plot* method [30]

Both micro- and mesoporous volumes of the biochars get a bigger volume with increasing pyrolysis temperature. Salt activator has a role for both of pore template and chemical activator during pyrolysis. As the pore template, the activator physically controls the pore volume of the biochar. Besides that, as the chemical activator, salt activator chemically improves the pyrolysis reaction [31]. The activator liquid facilitates the degradation of the precursor by attracting the water molecules to form the hydrated compound. And this at the end is released again

with elevated pyrolysis temperature [32]. $CoCl_2.6H_2O$ melts at 87 ºC and loses all its hydrate molecules in 120 – 140 ºC [33]. It means that $CoCl_2$ activator presents as liquid anhydrated salt at each pyrolysis temperature. The increasing temperature improves mobilization of the template liquid to form more porosity of the biochar. However, the pore volume of the biochar decreases again at pyrolysis 750 ºC. This may be affected by the more thermally condensed of aromatic carbon structures inside the biochars. Thermal condensation causes improvement of the aromatic cluster size and degree aromaticity at a higher pyrolysis temperature [24]. This phenomenon is also observed during the study, that pyrolysis at 750 ºC was slightly decreased the pore size of biochar. Pore size distribution of the biochars in **Figure 1** shows that all biochars have relatively the same height of peaks at about pore size of 50 Å.

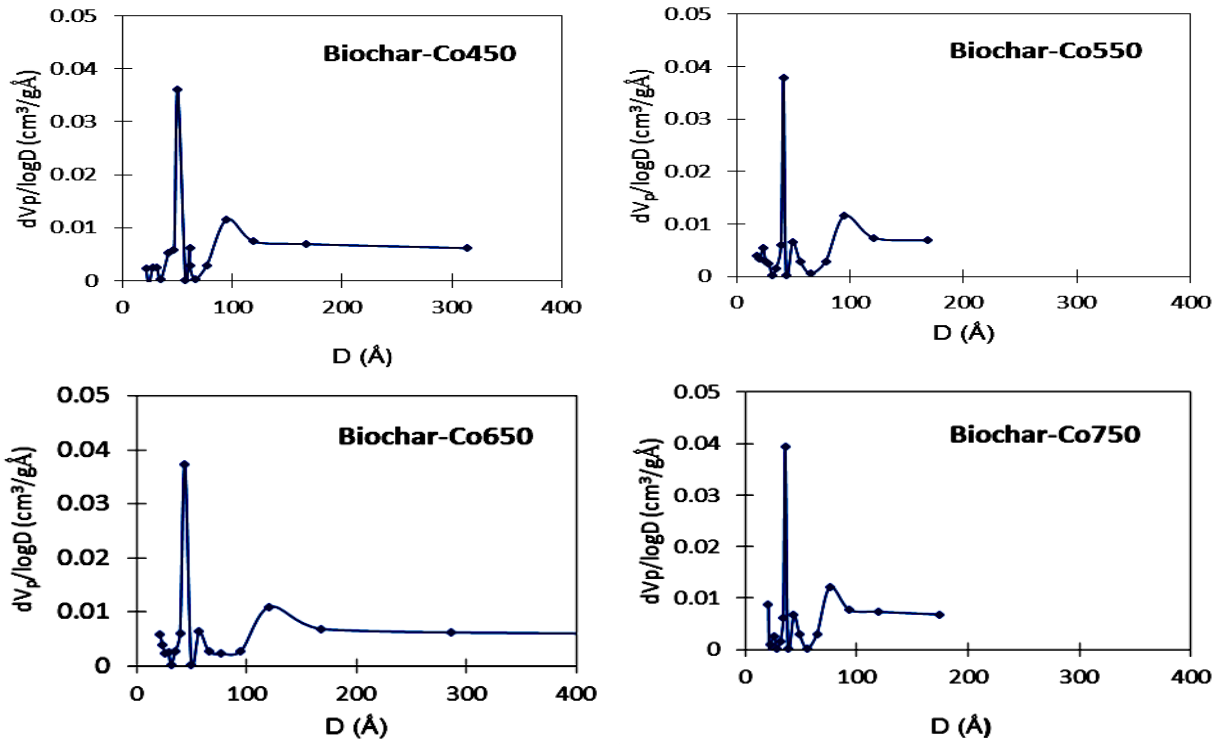

Figure 1. Pore size distribution of patchouli biochars using $CoCl_2$ activator at various pyrolysis temperatures

It means that all temperatures give relatively same pore uniformity. However, another peak (at 100 Å) increases by increasing temperature from 550 ºC to 650 ºC, and decreases again by increasing of temperature from 650 to 750 ºC. This changing is similar to that previously reported [24], the changing of pore volume which is caused by the aromatic structure condensation.

3.2 *Surface functional groups of biochars*

The surface functional group of biochars affect adsorption performance because it determines the polarity of biochars. The functional groups of patchouli biomass and the biochars prepared in various pyrolysis temperatures have been characterized using FTIR spectrophotometer. The structural changing easily observed due to the pyrolysis process. **Figure 2** shows the bands in 3410, 2997, 1614, and 1476 cm^{-1}. By comparing those spectra bands to that of activated carbons reported previously by other researchers [34, 35, 36, 37] indicate the important functional groups such as –OH hydroxyl of hydrate or surface hydroxide, C-H of an aliphatic hydrocarbon, C=O carbonyl or carboxyl, and C=C aromatic groups, respectively. Those spectra bands decrease by increasing of the pyrolysis temperature. It is due to a higher pyrolysis temperature dehydrated and or decarboxylated of biochar functional group, and then diminish their number in the surface of biochars.

Spectra bands of biochars (**Figure 2**) prepared at 350 and 450 °C using cobalt chloride activator are weaker than that prepared without activator. Besides that, significant changes of spectra of C=O and C-O bands disappear during pyrolysis 450 and 550 °C (with activator). But without the presence of cobalt chloride activator, these bands are not detected during pyrolysis at 550 and 650 °C. These facts indicate that cobalt chloride activator improves the pyrolysis reaction, and thus modify the surface with less polar functional groups. This affects the chemical properties of biochar become less polar.

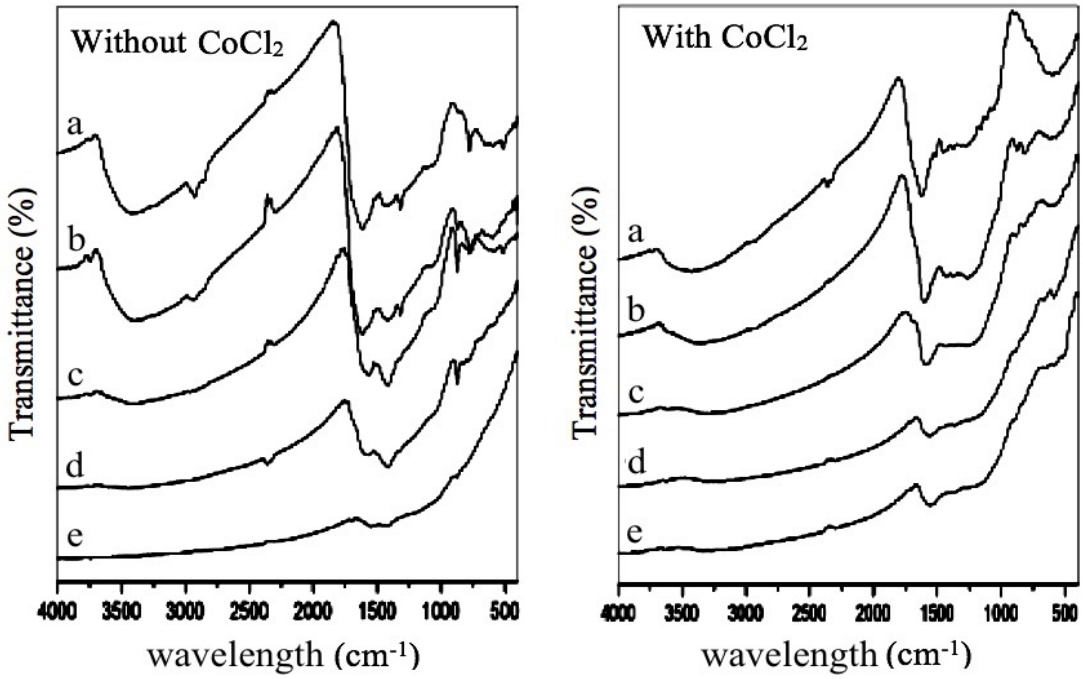

Figure 2. FTIR spectra of biochars prepared with and without $CoCl_2$ activator in various pyrolysis temperatures: a) 350 °C, b) 450 °C, c) 550 °C, d) 650 °C, and e) 750 °C

3.*3 Crystal structure of biochar*

Crystal structure of biochar has been characterized using X-ray diffraction method. The diffractograms of the biochars are reported in **Figure 3**. The biochar prepared at 450 and 750 °C were chosen for this characterization to show the effect of pyrolysis temperature on their changing of patterns.The biochars taken at pyrolysis temperature of 450 °C shows 2 peaks, i.e at $2\Theta \approx 22.55^{o}$ (d = 0.394 nm) and 45.55^{o} (d = 0.199 nm). The wide peaks indicate the amorphous structure [38]. Pattern of 2 peaks were similar to other product of biomass carbonizations, such as from rose petals [39], eucalyptus wood [40]. The main peak of the carbon diffractogram has the d_{002} value of 0.394 nm. It is larger than the d_{002} value of standard graphite data on JCPDS-ICDD card no 02-0456 ($2\Theta = 26.5^{o}$; d_{002} = 0.335 nm). This deviation indicates the disorder of graphite structure in the biochar. In the other side, the biochar which was prepared at the higher temperature (750 °C) shows reduction of wide peaks as shown by the biochar prepared at 450°C. It indicates that amorphous structure has been reduced by increasing temperature. However, some peaks emerge which was derived from some remaining activator, i.e as CoO as a result of the reaction between $CoCl_2$ and oxide gasses which were emitted along the pyrolisis process.

3.4 *Thermal analysis*

TGA and DTA characterizations have been conducted in order to predict chemical reaction during the pyrolysis process of patchouli biomass using $CoCl_2$ impregnation. The results are displayed in **Figure 4 and 5.** The analysis confirms of some results as follows:

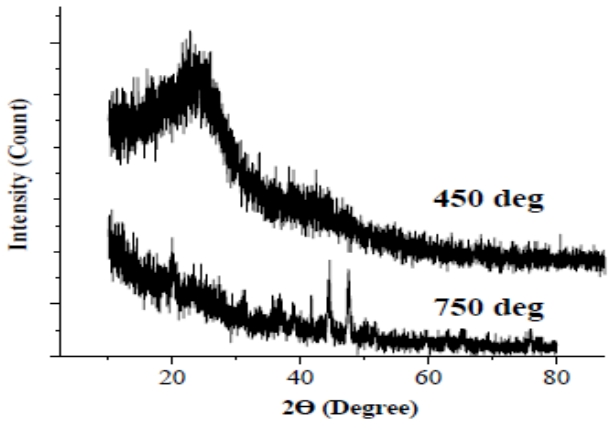

Figure 3. X-ray diffractogram of biochar prepared from patchouli biomass using $CoCl_2$ activator at 450 and 750 ^oC

1)Temperature 50 – 120 ^oC

TGA curve shows that $CoCl_2$ activator causes larger weight loss of mass than that prepared biochar sample without activator. It is probably related to dehydration reaction of patchouli biomass which has improved by the addition of $CoCl_2$. Cobalt chloride hexahydrate ($CoCl_2.6H_2O$) releases the hydrates in several steps; at 52-56 ^oC, four hydrates is decomposed, at 100 ^oC another H_2O is released, and between 120-140 ^oC, all hydrated structures of cobalt chloride decompose [33]. These changes are correlated to that of two endothermic peaks in DTA analysis (**Figure 5**). A sharper peak in TGA/DTA analysis, an indication that during pyrolysis, the involvement of cobalt chloride activator enlarges the heat flow. Conversely, the biochar's sample prepared without cobalt chloride activator give less sharpen peaks (**Figure 4 and 5**).

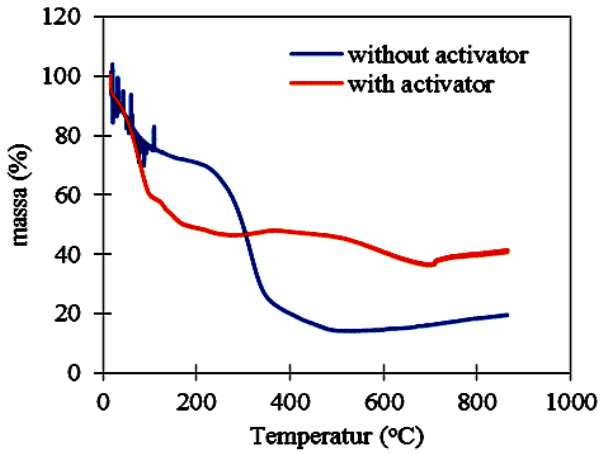

Figure 4. TGA analysis of patchouli biomass with and without $CoCl_2$ activator

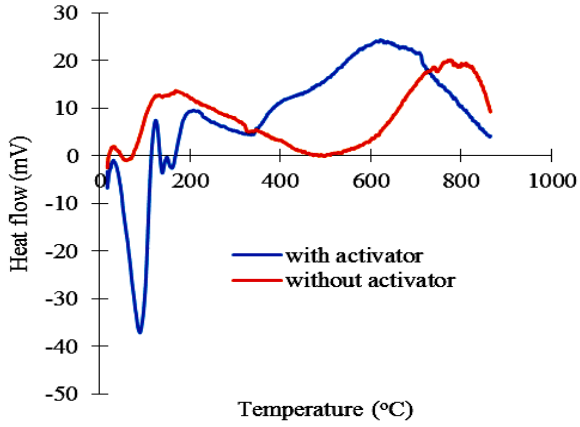

Figure 5. DTA analysis of patchouli biomass with and without $CoCl_2$

2) Temperature 120 – 250 ^oC

In this TGA temperature range (**Figure 4**), biochar sample prepared using cobalt chloride activator relatively loses a large mass than that prepared without activator. By comparing pattern of TGA curves for hemicellulose, cellulose, and lignin pyrolisis without activator, the little decreasing pattern of the curve from 120 to 250 ^oC is similar to each lignin and hemicellulose curves of TGA. This result inline to the DTA spectra in **Figure 5** which shows minimum peak (endothermic) and maximum peak

(exothermic) in range of 120 - 250°C. This peak correlates to the endothermic and exothermic peaks of lignin and hemicellulose [41]. Another possibility correlates to decomposition reaction of cobalt carbonate to cobalt oxide and CO_2 gas. This decompositon reaction is analogy of thermal decomposition reaction of $ZnCO_3$ [42]. Cobalt carbonate may be produced by thermal reaction of cobalt chloride activator and carbon dioxide gas which was evolved by pyrolysis reaction.

3) Temperature 250 – 500 °C

In this range of temperature, pyrolysis without activator shows larger decreasing of mass compared to that biochar prepared with the activator at range of 250 - 350°C and 350°C - 500°C. These change may be related to the decomposition of lignin/hemicellulose and cellulose, respectively. Those decreasing weight of biomass are related to minimum peak (endothermic) and maximum peak (exothermic) for decomposition of cellulose and lignin, respetively [41]. The smaller weight loses in pyrolysis of patchouli biochar prepared using activator indicates that cobalt chloride salt can prevent the formation of volatile substances during pyrolysis.

4) Temperature >500 °C

Weight loss of sample at about 730 °C may be related to decomposition of lignin [41]. Another possibility is decomposition of cobalt oxide to Co metal and oxygen gas thermally [43].

3.5. Adsorption test

The adsorption evaluation is undertaken using three different structures of commercially and commonly used of drug (paracetamol) and antibiotics (tetracycline and amoxicillin). All these molecules have both nonpolar and polar group and such as phenyl or aromatic groups and also hydroxyl, carbonyl, and amine groups (**Figure 7**). Four different concentrations of the drug are used with two times of repetition analysis. The purpose is to understand the correlation of porosity and functional groups on the biochar surface with their adsorption capability (**Figure 6**). The patterns of the graph in **Figure 6** show an increasing of q_e by increasing drug concentration or adsorbates. The adsorption value increases by a sequence of amoxicillin < tetracycline < paracetamol.

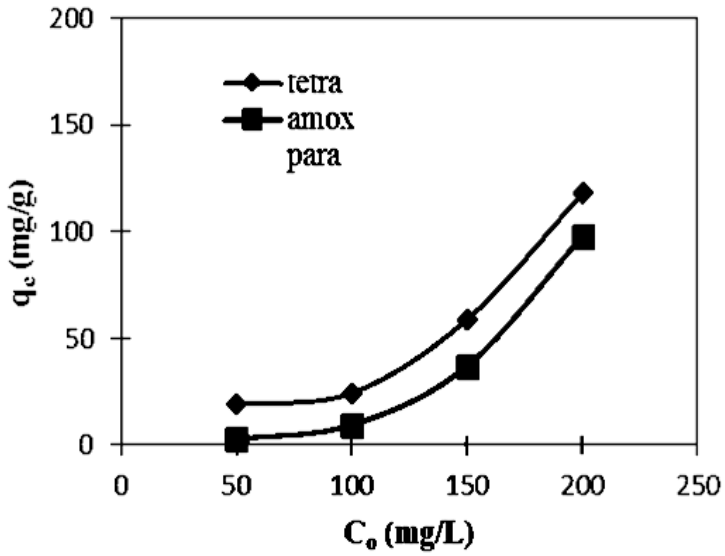

Figure 6. Adsorption values of drugs on the biochar at various initial concentrations

Paracetamol has active functional groups such as–OH, C=O, and NRArH. Tetracycline has –OH, C=O, NRH_2, $NArR_2$; meanwhile amoxicillin –OH, -NH_2 ,-NH, and -COOH functional groups [33]. These groups have Lewis base atoms which can interact with functional groups from patchouli biochar by using hydrogen bonding or Van der Waals force interaction. The number of functional groups increases from paracetamol < amoxicillin < tetracycline, respectively. In addition to that, the nonpolar interaction of the drug with biochar can undergo through Van der Waals force interaction. Based on the molecule shapes [33], paracetamol has the shortest structure, tetracycline has a long structure, and amoxicillin has the bend long structure. This condition makes the highest adsorption could be achieved in paracetamol. The bent structure of amoxicillin seems to become a reason for the lowest adsorption in biochar.

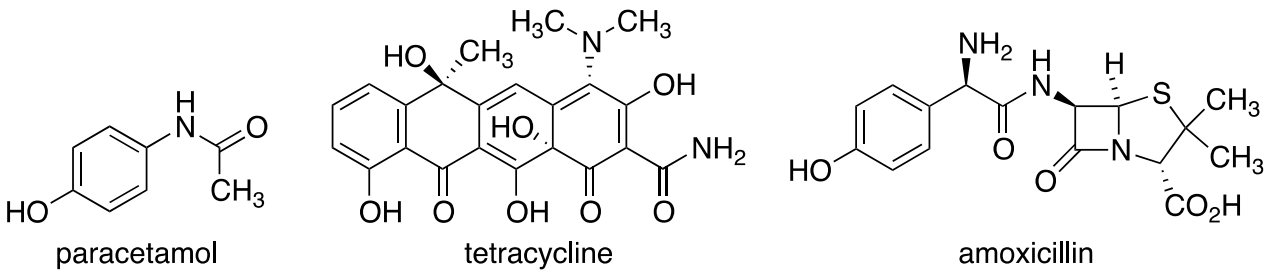

Figure 7. Chemical structures of drugs [33]

4. Conclusions

Biochars have been prepared from patchouli biomass using $CoCl_2$ activator in various temperatures (350-750 ^oC). Biochar prepared at 450 ^oC give the highest microporosity and largest BET surface area, but preparation at 650^oC provides the highest mesoporosity and total pore volume. All biochars prepared have a pore size distribution in about 5 nm. The polar functional groups of biochar disappear at 650 ^oC and 750 ^oC of pyrolysis.

Acknowledgments

The authors would like to thank DIKTI for PUPT project (No.033/SP/2H/LT/DRPM/II/2016) of research [44]. We also thank to Department of Chemistry, Brawijaya University, which has provided the laboratory for conducting this research.

References

1. S. Shenbagavalli, and S.Mahimairaja, "Production and Characterization of Biochar from Different Biological Wastes", *Int. J. Plant Anim. Environ. Sci*, 2 (2013) 197-201.
2. K. Jindo, H.Mizumoto, Y.Sawada, M.A.Sanchez-Monedero, and T.Sonoki, T., "Physical and Chemical Characterization of Biochars Derived from Different Agricultural Residues", *Biogeosci*, 11 (2014) 6613–6621.
3. A.U. Rajapaksha, M.Vithanage, M. Zhang, M.Ahmad, D. Mohan, S.X.Chang, Y.S. Ok, "Pyrolysis Condition Affected Sulfamethazine Sorption by Tea Waste Biochars", *Bioresour. Technol*., 166 (2014) 303–308.
4. A. Budai, L.Wang, M.Gronli, L.T. Strand, M.J. Antal, J.S.Abiven, A.Dieguez-Alonso, A. Anca-Couce, D.P. Rasse, "Surface Properties and Chemical Composition of Corncob and Miscanthus Biochars: Effects of Production Temperature and Method", *J. Agric. Food Chem*., 62 (2014) 3791–3799.

5. K.N.W. Sum, "Adsorption of Trimethyltin, Arsenic (V), Zinc and Copper by Palm Oil Mill Sludge Biochar Prepared by Microwave", A project report of the bachelor degree, Faculty of Engineering and Green Technology, Universiti Tunku Abdul Rahman (2016).
6. A. Krismawati, "Nilam dan Potensi Pengembangannya : Kalteng Jadikan Komoditas Rintisan", Tabloid Sinar Tani (2005).
7. G. Garrote, J. Dominguez, C. Parajo, "Hydrothermal Processing of Lignocellulosic Materials", Holz als Roh- und Werkstoff, 57 (1999) 191-202.
8. E. Kim, C.Jung, J. Han, N.Her, C.M.Park, A. Son, Y.Yoon, "Adsorption of Selected Micropollutants on Powdered Activated Carbon and Biochar in The Presence of Kaolinite". *Desalination and Water Treatment* (2016) 1-13.
9. K. Jindo, H. Mizumoto, Y. Sawada, M.A. Sanchez-Monedero, and T. Sonoki, "Physical and Chemical Characterization of Biochars Derived from Different Agricultural Residues" *Biogeosci.*, 11 (2014) 6613–6621.
10. X. Gai, H.Wang, J. Liu, L.Zhai, S.Liu, T.Ren, and H.Liu, "Effects of Feedstock and Pyrolysis Temperature on Biochar Adsorption of Ammonium and Nitrate", *PLoS One*., 9 (2014) 1-19.
11. X. Yu, A.Qin, L. Liao, R.Du, N.Tian, H.Huang, and C.Wei, "Removal of Organic Dyes by Nanostructure ZnO-Bamboo Charcoal Composites with Photoctalaysis Function", *Adv.Mater. Sci.Eng.*(2015) 1-6.
12. M. Agarwal, J. Tardio, and S.V.Mohan, "Pyrolysis Biochar from Cellulosic Municipal Solid Waste as Adsorbent for Azo Dye Removal: Equilibrium Isotherms and Kinetics Analysis", *Int. J. Environ. Sci. Dev.*, 6 (2015) 67-72.
13. M. Uchimiya, I.M. Lima, K.T.Klasson, L.H.Wartelle, "Contaminant Immobilization and Nutrient Release by Biochar Soil Amendment: Roles of Natural Organic Matter Minori", *Chemosphere*, 80 (2010) 935–940.
14. J. Jiang, "Progress of Biochar Supercapacitors", 1st Midwest Biochar Conference, Illionis Sustainable Technology Center, June 14 (2013).
15. M.M. Sihabudeen, A.A. Ali, and A.Z. Hussain, "Removal of Heavy Metals from Ground Water Using Eucalyptus Carbon as Adsorbent", *Int.J. ChemTech Res.*, 9 (2016) 254-257
16. J. Paz-Ferreiro, H.Lu, S. Fu, A. Méndez, and G. Gascó, "Phytoremediation and Biochar to Remediate Heavy Metal Polluted Soils: A Review, Agriculture, Ecosystems and Environment", *Solid Earth*, 5 (2014) 65–75.
17. A.A.T. Kamal, C.J. Atkinson, A. Khan, K. Zhang, P.Sun, S. Akther, Y. Zhang, "Biochar Remediation of Soil: Linking Biochar Production With Function in Heavy Metal Contaminated Soils", *Plant, Soil and Environment*, 67 (2021) 183–201.
18. S. Ismadji, D.S.Tong, F. Edi, Soetaredjo, A.Ayucitra, W.H. Yu, C.H. Zhou, "Bentonite-hydrochar Composite for Removal of Ammonium from Koi Fish Tank", *Appl. Clay Sci.*, 114 (2015) 467–475.
19. L. Xiao, E.Bi, B. Du, X.Zhao, C.Xing, "Surface Characterization of Maize-Straw-Derived Biochars and Their Sorption Performance for MTBE and Benzene", *Environ. Earth Sci.*, 71 (2014) 5195–5205.
20. F. Lian, Z.Song, Z. Liu, L. Zhu, B. Xing, "Mechanistic Understanding of Tetracycline Sorption on Waste Tire Powder and Its Chars as Affected by Cu (II) and pH", *Environ. Pollut.*, 173 (2013) 264-270.

21. T. Setianingsih, Masruri, B. Ismuyanto, "Study of Chemical Activator in Preparation of Biochar Adsorbent from Patchouli Biomass for Removing Drug Contaminant", *Int.J. ChemTech Res.*,10 (2017) 10-19.
22. R. Rostamian, M. Heidarpour, S.F. Mousavi, and M. Afyuni, "Characterization and Sodium Sorption Capacity of Biochar and Activated Carbon Prepared from Rice Husk", *J. Agr. Sci. Tech.,* 17 (2015) 1057-1069.
23. M.Wis´niewski, A. Pacholczyk, A.P. Terzyk, G.Rychlicki, "New Phosphorus-containing Spherical Carbon Adsorbents As Promising Materials in Drug Adsorption and Release",. *J.Colloid Interface Sci.* 354 (2011) 891–894.
24. J. Park, I. Hung, Z. Gan, O.J. Rojas, K.H. Lim, S. Park., "Activated carbon from biochar: Influence of its physicochemical properties on the sorption characteristics of phenanthrene" *Bioresour. Technol.* 149 (2013) 383–389.
25. L. Hernandez-mena, A.Pécora, A. Beraldo, "Slow Pyrolisis of Bamboo Biomass: Analysis of Biochar Properties", *Chem. Eng. Trans.*, 37 (2014) 115-120.
26. N. Oumam, M. Oumam, A.K.Abourriche, A.M. Abourriche, H. Hannache, and A. Bennamara, "Elaboration and Characterization of A New Activated Carbon Obtained from Oregano Residue: Application in Environmental Field", MATEC Web of Conferences 5 (2013).
27. E. Moosavi, S.Dastgheib, and R.Karimzadeh, "Adsorption of Thiophenic Compounds from Model Diesel Fuel Using Copper and Nickel Impregnated Activated Carbons, *Energies*, 5 (2012) 4233-4250.
28. B. Chen, Z. Chen., L.Shafoang., "A Novel Magnetic Biochar Efficiently Sorbs Organic Pollutants and Phosphate, *Bioresour. Technol.*, 102 (2011) 716.
29. D.W. Cho, S., Kim, Y.F. Tsang, H. Song, "Preparation of Nitrogen-doped Cu-biochar and Its Application into Catalytic Reduction of *p*-nitrophenol", *Environ. Geochem. Health* (2017) 1-7.
30. S. Lowell and J.E.Shields, "Powder Surface Area and Porosity". 2nd ed. Chapman and Hall Ltd. New York, 2004.
31. S. Huang, S. Zuo, Z. Xu, C. Hana, and J. Shen, "Mesoporous Carbon Prepared from Carbohydrate with A Metal Chloride Template", *J. Mater. Chem*., 19 (2009) 7759–7764
32. H. Marsh and F. Rodriguez-Reionoso, "Activated Carbon, Elsevier Ltd (2006) 331.
33. M. Windolz, S. Budavari, R.F. Blumeti, E.S. Otterbein, Preparation of Activated Carbon Using the Copyrolysis of Agricultural and Municipal Solid Wastes at a Low Carbonization Temperature, The Merc Index : An Encyclopedia Of Chemicals, Drugs, and Biologicals, Merck & CO, Inc., 10th ed., USA(1983).
34. M. Sevilla and A.B. Fuertes, "The Production of Carbon Materials by Hydrothermal Carbonization of Cellulose", *Carbon*, 47 (2009) 2281–2289.
35. Z. Song-lin , G.A.O.Shang-yu , G.A.O., Xi-gen, Y., Bo-sen,U. Carbonization Mechanism of Bamboo (phyllostachys) by Means of Fourier Transform Infrared and Elemental Analysis, *J.Forest. Res.*, 14 (2003) 75-79.
36. A.C. Lua and T.Yang, " Characteristics of Activated Carbon Prepared From Pistachio-Nut Shell by Zinc Chloride Activation Under Nitrogen and Vacuum Conditions", Journal of Colloid and Interface Science, *J. Colloid Interface Sci.*, 290 (2005) 505–513.
37. P.K. Chayande, S.P. Singha, M.K.N. Yenkie, "Characterization of Activated Carbon Prepared from Almond Shells for Scavenging Phenolic Pollutants", *Chem Sci Trans*., 2 (2013) 835-840.
38. C. Chen, X. Sun, X. Jiang, D. Niu, A.Yu, Z. Liu, J.G. Li, "A Two-Step Hydrothermal Synthesis Approach to Monodispersed Colloidal Carbon Spheres", *Res. Lett.*, 4 (2009) 971–976.

39. N. IIkhtiarini, R.T. Tjahjanto, T. Setianingsih, "The Effect of Parameter Combinations (Carbonization Temperature Chemical Activator) on Degree of Graphitization, Aromaticity, and Fungsional Group of Rose Petal (Rosa sp) Based-Activated Carbon", IOP Conf. Series: Materials Science and Engineering", 546 (2019) 1-8.
40. B.C.C. Fernandes, K.F. Mendes, "Impact of Pyrolysis Temperature on the Properties of Eucalyptus Wood-Derived Biochar", *Materials*, 13 (2020) 1-13.
41. H. Yang, R. Yan, H.Chen, D.H. Lee, "Characteristics of Hemicellulose, Cellulose, and Lignin Pyrolisis", *Fuel*, 86 (2007) 1781–1788.
42. S. DeMeo, "The Decomposition of Zinc Carbonate: W Using Stoichiometry To Choose between Chemical Formulas", *Journal of Chemical Education*, 81(2004) 119-120.
43. B.V. L'vov, "Mechanism of Carbothermal Reduction of Iron, Cobalt, Nickel and Copper Oxides" *Thermochimic. Acta* , 360 (2000) 109-120.
44. T. Setianingsih, Masruri, B. Ismuyanto, "Adsorben Unggul Komposit Biochar-Metal Berbasis Limbah Padat Nilam Untuk Meminimasi Kontaminan Air Dalam Menunjang Ketersediaan Air Berkelanjutan", *Laporan PUPT*, Universitas Brawijaya Malang (2016).

(2021) ; http://www.jmaterenvironsci.com